

Influence of soft rime ice severity on conductor audible noise characteristics of positive corona discharge

Gaohui He^{1,2}, Qin Hu¹, Lichun Shu¹, Xingliang Jiang¹, Hang Yang¹, Dachuan Yang¹
and Raji Sundararajan²

1. State Key Laboratory of Power Transmission Equipment & System Security and New Technology, Chongqing University, China

2. School of Electrical Engineering Technology, Purdue University, USA

phone: (1) 765-775-3876

e-mail: hegaohui@cqu.edu.cn

Abstract—With large-scale construction of extra-high voltage (EHV) and ultra-high voltage (UHV) DC transmission lines and frequent foul weather, such as icing, corona generated audible noise (AN) during foul weather conditions have attracted widely attentions. In this research, audible noise characteristics of soft rime ice-covered, smooth conductor, influenced by icing severity are studied. The 37.6 mm diameter specimen located in a corona cage is energized with positive polarity voltage during artificial icing. Both the conductor diameter and the applied icing electric field intensity are analogous to these of ± 500 kV and ± 800 kV DC transmission line configuration in China. Test results show that an increase of icing severity leads to a higher AN. Studies of the 1/3 octave band spectrum indicate that the 353 Hz divides the noise spectrum into two bands. With the increasement of corona discharge intensity, the differences between the A-weighted AN and sound pressure levels of frequency components are constant, while the lower frequency components in background noise band are stable. Furthermore, the proposed 3.15 kHz component extraction method is useful for the audible noise separation from long term transmission line audible noise monitoring, and with an uncertainty of less than 1 dB.

I. INTRODUCTION

Conductor selection is one of the most important decisions faced by transmission line designer. The conductor size is often established by corona performance [1], including corona loss (CL), AN and radio interference (RI) for DC transmission lines [2], especially for the design of EHV and UHV transmission lines [3]. However, the cost and workload of EHV and UHV test lines are huge and hard to simulate extreme weather conditions. Corona cages are widely used to investigate the conductor AN characteristics, affected by precipitations [4], atmospheric pressure [5] and conductor surface conditions [6, 7].

With the construction of UHV DC transmission project in China, the operating 13 UHV DC projects are inevitably crossing cold regions. Besides, bundled conductors used in EHV and UHV transmission lines are subjected to greater ice and wind loadings than single conductors of the same total cross section [2]. On the other hand, public's psychological

reactions to the same noise in different ambient conditions shall be taken into account, especially the ambient noise level and the weather conditions. Experiences show that the AN in light rain, fog, mist, snow, or just after a rain while the conductors are still wet are more objectionable [2, 8], whose background noise are relatively low, which is also suitable for icing weather conditions. Due to the differences in the spectral composition, the recommended threshold for AN produced by AC transmission line is 55 dB(A), while it is a reduced 50 dB(A), for DC transmission line, which is much less than that of traffic noise, 62 dB(A). Hence, it is practical interest to study the AN of DC transmission line subjected to icing weather conditions. However, the existing corona researches of icing conditions are mainly concentrate on the corona inception voltage and CL of AC transmission lines [9-14].

Random nature of HVDC transmission line AN is the reason that in practice the best determination of AN level is obtained from the continuous monitoring procedures. An automatic interference filtration method is needed due to the great volume of the recording and stored continuous signal. Literature [15] finds that the L_{50} (the noise level exceeds for 50% of the measurement period) value for estimation of the long-term levels during rain leads to satisfactory results. In [16], the 8 kHz component plus 11 dB is used to separate the audible noise from background noise during fine weather conditions.

II. THEORETICAL BACKGROUND

A. Positive Corona Discharge

Ionization in the positive corona cannot be provided by the cathode phenomena, because, in this case, the electric field at the cathode is very low. Here, ionization processes are related to the formation of the positive streamer. Corona inception conditions can be described for the positive corona (1), using the criteria of positive streamer formation (Meek breakdown criterion), taking into the nonuniformity of the corona and contributions of electron attachment [17] as:

$$\int_0^{x_{\max}} [\alpha(x) - \beta(x)] dx \approx 18-20 \quad (1)$$

where, $\alpha(x)$ and $\beta(x)$ are the first and second Townsend coefficients, describing ionization and electron attachment, respectively, x_{\max} corresponds to the distance from the anode.

The positive corona discharge has three distinct forms, that is burst corona mode, positive glow and positive pre-breakdown streamers. From long terms of operating experiences, its known that the audible noise of bipolar high voltage DC transmission lines is mainly generated from positive polarity.

B. Sound Generation and Propagation

Sound is the sensation produced at the ear by very small pressure fluctuations in the air. In the case of audible noise, the pressure fluctuations are generated by the collision of charged particles. Both positive corona modes, the burst corona mode and pre-breakdown streamer mode, comprise repetitive transient discharges in which rapid ionization and movement of space charges take place in a very short interval of time, of the order of milliseconds and hundreds of nanoseconds, respectively [18]. The movement at very high

speeds, particularly of the electrons created in the discharge, results in the transfer of kinetic energy to neutral air molecules through collisions, this sudden transfer of energy during a short interval of time is equivalent to an explosion taking place at the corona site, giving rise to the generation of a transient acoustic wave [1].

The acoustic potential function, φ , is defined so that its negative gradient provides the particle velocity, \mathbf{u} , as (2):

$$\mathbf{u} = -\nabla\varphi \quad (2)$$

Equations (3) and (4) give the derivatives, as

$$p = \rho \frac{\partial\varphi}{\partial t} \quad (3)$$

where, p is the acoustic pressure, t is the time.

$$\nabla^2\varphi = (1/c^2)\partial^2\varphi/\partial t^2 \quad (4)$$

For gases, the speed of sound depends upon the temperature of the gas through which the acoustic wave propagates. The speed of sound can be calculated by (5):

$$c = 331 + 0.61T \quad (5)$$

where, c is the speed of sound, in m/s; T is the temperature of the gas, in °C.

III. TEST ARRANGEMENT

A. Specimen and Corona Cage

The artificial icing and corona tests presented in this research are performed in a corona cage installed inside a multifunctional artificial climate chamber [14]. The circular-section corona cage with a diameter of 1 m is composed of a 2 m length measuring section and two 0.3 m length guard sections.

The specimen used in the tests, a smooth conductor (metallic tube), have a length of 3.5 m and diameter of 37.6 mm, which is analogous to ACSR-720/50, the sub-conductor used in ‘Xiangjiaba-Shanghai ±800 kV UHV DC demonstration project’ in China [19]. The coaxial arranged specimen is suspended by two 110 kV post insulators, and the applied voltages are measured by a high voltage resistance divider with a precision of 2%. To eliminate the discharge beyond the measuring section, two metallic balls are installed at both ends of specimen, and power source is applied to the conductor via a corona-free high voltage lead wire.

B. Artificial Icing

Purified and deionized tap water is supplied to the industrial chiller to produce freezing water before tests, the conductivity and temperature of the prepared freezing water is 27 $\mu\text{S}/\text{cm}$ ($\pm 5 \mu\text{S}/\text{cm}$) (corrected to 20°C) and 5.0 °C respectively. The room temperature of the artificial multifunctional climate room is set to -11~-14°C, after precooling for half an hour to achieve a thermal equilibrium between the specimen and the ambient temperature. A 136.9 kV positive polarity DC voltage is applied to the specimen, corresponding to electric field intensity of 22.2 kV/cm, which is equal to the conductor surface gradient of practical UHV project, and the spray system is turn on at the same time. 11 air atomizing nozzles used in [13] are adopted in the spray system to produce fine water droplets, distributed

uniformly around the conductor surface, and the nozzles are mounted at $45^\circ \pm 5^\circ$ to the horizontal.

The icing thickness and icing weight are measured after corona tests, the results are listed in Table 1. And two icing severities are considered in this research, namely 15 mm medium ice and 20 mm heavy ice, which are common considered during the design of transmission lines.

TABLE 1: THE ICING PARAMETERS OF DIFFERENT ICING SEVERITY

	Icing severity 1	Icing severity 2
Ice region	15 mm medium ice region	20 mm heavy ice region
Icing thickness	11.4 mm	17.5 mm
Icing weight	169.7 g/m	481.7 g/m

C. Audible Noise Measurement

A class 1 sound level meter (AWA6228+) which conforms to IEC standard 61672-1 [20] is used in the tests, “fast” mode with a time constant of 125 milliseconds is chosen and is designed to approximate the response of the ear. It is mounted on a tripod and is 1.5 m above the ground, locates at the center of the span and orients towards the specimen (adjusting it for maximum reading) in a plane normal to it. Insertion loss is not considered since wind cover is not used during tests. And an acoustic calibrator is used before and after each series of sound-pressure level measurement.

The distance from the sound level meter to the conductor surface is 0.65 m, which is smaller than the critical distance r_c of the multifunctional artificial climate chamber, 0.69 m, calculated according to (6), namely the reverberant sounds are ignorable compared with the direct sound [21].

$$r_c = \frac{1}{4} \sqrt{R / \pi} \quad (6)$$

where, R is the room constant, 23.68, calculated according to (7):

$$R = S \bar{\alpha}^* / (1 - \bar{\alpha}^*) \quad (7)$$

where, S is the surface area of the room, 450 m²; $\bar{\alpha}^*$ is the mean absorption and equivalent absorption coefficient, 0.05, for the multifunctional artificial climate chamber.

IV. RESULTS AND DISCUSSION

A. The A-Weighted Sound Pressure Level

The random discharge nature of DC corona causes AN spectrum to be broadband or fluctuating, and the simplest and most popular method for rating such noise intrusions is to rely upon some measure of the average sound level magnitude over time. The A-weighted energy-equivalent sound level ($L_{A,eq}$) is used as a descriptor of both occupational and environmental noise and for an average over time [22], (t_2-t_1). It is the average of the A-weighted sound energy level of a fluctuating noise over a specified period of time, mathematically, the equivalent sound level is defined in [18] as (8):

$$L_{A,eq} = 10 \log_{10} \left[\frac{1}{(t_2 - t_1)} \int_{t_1}^{t_2} \frac{p^2(t)}{p_{ref}^2} dt \right] \quad (8)$$

where, $p(t)$ is the time-varying A-weighted sound level, in μPa ; p_{ref} is the reference pressure, $20 \mu\text{Pa}$; $(t_2 - t_1)$ is the time period of interest, 10 seconds in this research.

For the background noise is the factor most likely to affect sound pressure level readings. If the differences between the background noise L_B and the total measured sound pressure level L_M are range from 3 dB to 10 dB, that is $3 \text{ dB} < L_M - L_B < 10 \text{ dB}$, a correction must be made according to [22]. If the difference is less than 3 dB a valid sound test probably cannot be made. It should be pointed out that the AN may still be audible even the level is similar to ambient due to its unique frequency characteristics.

The A-weighted energy-equivalent sound levels ($L_{A,eq}$) of different icing severities are plotted in Fig. 1. The measured experimental values of icing severity 1 and 2 are plotted by triangles and circles, respectively. And the values in shaded area are not discussed in this research according to the 3dB rule stated above. As the enlargement of the applied voltage, the audible noise curves of both icing severities are of hyperbolic type. The best fitted mathematical expressions are given by (9) and (10) and are plotted in Fig. 1 in solid lines.

$$\text{Icing severity 1: } L_{A,eq} = 126.4 - 8349/U \quad (9)$$

$$\text{Icing severity 2: } L_{A,eq} = 123.3 - 7712/U \quad (10)$$

where, U is the applied voltage, in kV; $L_{A,eq}$ is A-weighted energy-equivalent sound level, in dBA.

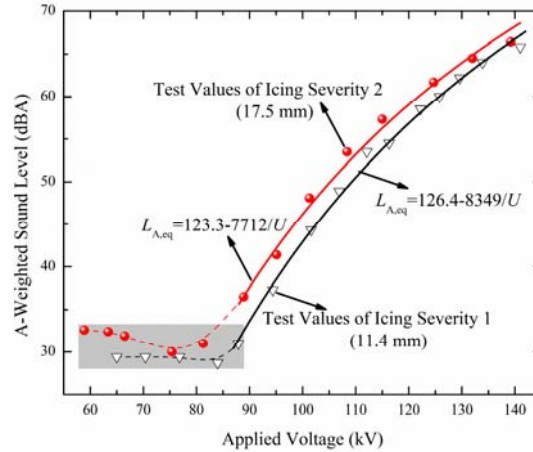


Fig. 1. Influence of icing severity on A-weighted energy-equivalent sound level of soft rime ice-covered conductor (values in shaded area are not critical)

Although the growth of icing severity enlarges the conductor diameter, the AN of soft rime ice-covered conductor of icing severity 2 are about 1.5 - 4 dB higher. This is attributed to the enlargement of conductor surface area, which will lead to an augment of ice-tree

number. The tips of soft rime ice-tree distort the electric field serious [11], the effect of bigger quantities of discharge points predominates that of conductor diameter growth.

B. The Spectrum of Audible Noise

The human ear reaction to noise is too complicated to express by a single number. 1/3 octave band analysis is selected to study spectrum because it provides a further in-depth look into noise levels across the frequency composition. The 1/3 octave spectrums of background noise and three corona intensities of icing severity 1 are given in Fig. 2.

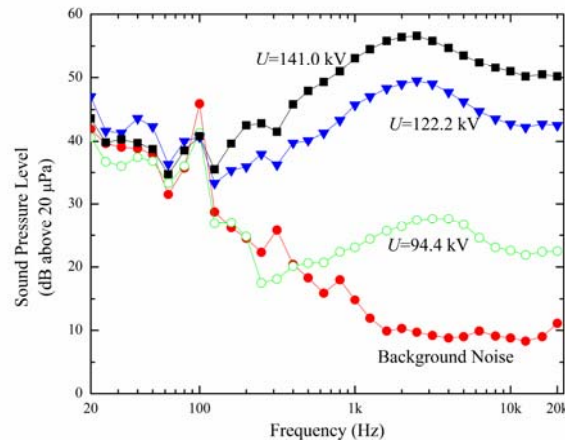


Fig. 2. The 1/3 octave spectrum of background noise and three different corona intensities of soft rime ice-covered conductor under icing severity 1

Unlike the audible noise of AC corona is composed by broadband noise and $2f$ -component [23] known as hum, the AN of DC transmission lines is a broadband noise. Since the 100 Hz hum is hardly attenuated even when passes through structures [2], the 100 Hz component of high voltage power supply is still existing in Fig. 2. The 100 Hz component of background noise is even higher than that of other corona intensities, which exclude the possibility of generating from DC corona discharge. In general, the sound pressure level of bigger frequency component is smaller for the background noise. When positive polarity voltage is introduced, the sound pressure levels of high frequency components grow significantly. The spectrums of higher corona discharge intensity ($U=122.2$ kV and $U=141.0$ kV) first increase then decrease, reaching their peak at 2.5 kHz.

A further analysis of the frequency components variation pattern finds that the audio frequency (usually range from 20 Hz to 20 kHz) could be divided into two bands, namely background noise band and corona discharge band. Characteristic frequency components in two band and A-weighted AN vary with applied voltage are plotted in Fig. 3.

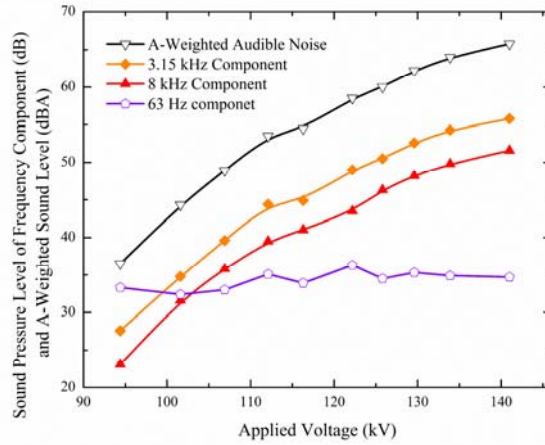


Fig. 3. A-weighted AN and characteristic 1/3 octave frequency components versus applied voltage under icing severity 1

In the background noise band, from 20 Hz to 353 Hz (the upper band limit when the 1/3 octave band center frequency is 315 Hz), the frequency components of AN keep unchanged with the increase of corona intensities (63 Hz component showed in Fig. 3). While in the corona discharge band, from 353 Hz to 20 kHz, the differences between frequency components and the A-weighted AN are a constant, C , with the growth of corona discharge intensity (3.15 kHz and 8 kHz component showed in Fig. 3). Among the frequency components in corona discharge band, the standard error of the constant C of 3.15 kHz is the minimum, 0.6 dB, and the relationship are given in (11):

$$L_A = H_{3.15\text{kHz}} + 10.1\text{dB} \quad (11)$$

where, L_A is audible noise, in dBA; $H_{3.15\text{kHz}}$ is the 3.15 kHz component of measured value, in dB.

The found relationship, (13) solve the problem of huge volume of data and ambient noise interference in long-term audible noise measurements. It can extract corona generated AN fast and accurately. Comparison of the recommended 3.15 kHz component method, the 8 kHz prediction method in [16] and the measured A-Weighted AN are made in Fig. 4.

The solid circles represent the measured A-Weighted audible noise values. The triangles stand for the predicted results of the proposed 3.15 kHz component extraction method in this research. And the hollow circles are the results of 8 kHz prediction method in [16]. Besides, the dash and solid lines represent the results of icing severity 1 and 2, respectively. it can be inferred that the proposed 3.15 kHz component extraction method is more precise.

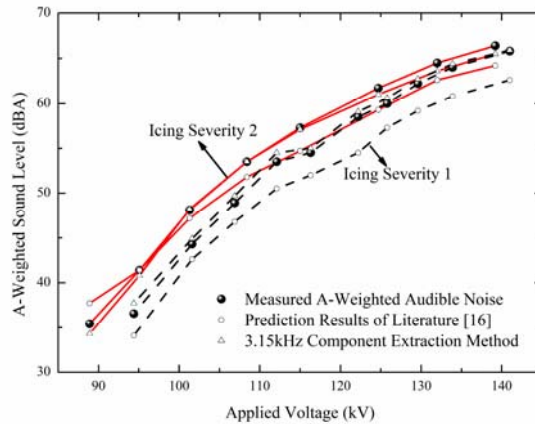


Fig. 4. Comparison of the measured A-weighted audible noise, the proposed 3.15 kHz component extraction method and 8 kHz prediction method of literature [16] under different icing severities

V. CONCLUSION

Through elaborated artificial energized icing process, soft rime icing with two icing severities are formed on a smooth conductor, which is analog to the sub-conductor used in operating EHV and UHV DC project. The widely adopted A-weighted energy-equivalent sound level ($L_{A,eq}$) and 1/3 octave band analysis method are used in this research. The following conclusions can be drawn out:

- With the augment of icing severity, namely the icing thickness for soft rime, the AN is bigger when the applied voltage is the same. And the A-weighted energy-equivalent sound level ($L_{A,eq}$) versus applied voltage is a hyperbola type curve.
- The AN spectrum of soft rime ice-covered conductor energized with positive polarity voltage is broad noise as expected, and the high frequency components are predominant at the operating voltage, the peak value appears around 2.5 kHz.
- The audio frequency could be divided into background noise band (20 Hz – 353 Hz) and corona discharge band (353 Hz – 20 kHz). In corona discharge band, the differences between the A-weighted AN and sound pressure levels of frequency components are constant. While the sound pressure levels in background noise level are independent of corona discharge intensities.
- 3.15 kHz component extraction method is recommended to filter the ambient interference during long-term AN measurement.

VI. ACKNOWLEDGEMENT

This work is supported by State Grid Chongqing Electric Power Company (SGCQDK00PJJS1600049), National Natural Science Foundation of China (51321063) and 111 Project. And G. He thanks financial support from China Scholarship Council (CSC).

REFERENCES

- [1] P. S. Maruvada, *Corona Performance of High-Voltage Transmission Lines*. Hertfordshire: Research Studies Press, 2000.
- [2] G. E. C. Transformer Laboratories and G. E. C. Electric Utility Systems Engineering Dept., *Transmission Line Reference Book: 345 kV and Above*. Palo Alto: Electric Power Research Institute, 1975.
- [3] W. Zhao, *HVDC Transmission Engineering Technology*. Beijing: China Electric Power Press, 2010. (in Chinese)
- [4] G. W. Juette and L. E. Zaffanella, "Radio noise, audible noise, and corona loss of EHV and UHV transmission lines under rain: Predetermination based on cage tests," *IEEE Transactions on Power Apparatus and Systems*, vol. PAS-89, pp. 1168-1178, 1970.
- [5] J. Tan, J. He, Y. Liu, Y. Yang, and Y. Chen, "Test results and analysis of altitude-change effect on audible noise of AC corona occurring on conductors with corona-test cage," *Proceedings of the CSEE*, vol. 30, pp. 105-111, 2010. (in Chinese)
- [6] X. Li, X. Cui, T. Lu, W. Ma, X. Bian, D. Wang, and H. Hiziroglu, "Statistical characteristic in time-domain of direct current corona-generated audible noise from conductor in corona cage," *Phys. Plasmas*, vol. 23, pp. 033503, 2016.
- [7] Y. Yi, Y. Wang and L. Wang, "Conductor surface conditions effects on audible noise spectrum characteristics of positive corona discharge," *IEEE Transactions on Dielectrics and Electrical Insulation*, vol. 23, pp. 1872-1878, 2016.
- [8] J. L. Fletcher and R. G. Busnel, *Effects of Noise on Wild Life*. New York: Academic Press, 1978.
- [9] X. Jiang, J. Chen, L. Shu, Z. Zhang, J. Hu, and S. Wang, "Study on the effects of glaze icing on the corona onset characteristics of stranded conductors," *IEEE Transactions on Dielectrics and Electrical Insulation*, vol. 21, pp. 704-712, 2014.
- [10] Q. Hu, T. Li, L. Shu, and X. Jiang, "Dynamic characteristics of the corona discharge during the energized icing process of conductors," *IET Generation Transmission & Distribution*, vol. 7, pp. 366-373, 2013.
- [11] X. Jiang, J. Chen, L. Shu, J. Hu, Z. Zhang, and S. Wang, "Studying corona onset characteristics after rime ice accumulation on energized stranded conductors," *IEEE Transactions on Dielectrics and Electrical Insulation*, vol. 20, pp. 1799-1807, 2013.
- [12] F. Yin, M. Farzaneh and X. Jiang, "Corona investigation of an energized conductor under various weather conditions," *IEEE Transactions on Dielectrics and Electrical Insulation*, vol. 24, pp. 462-470, 2017.
- [13] F. Yin, M. Farzaneh and X. Jiang, "Laboratory investigation of AC corona loss and corona onset voltage on a conductor under icing conditions," *IEEE Transactions on Dielectrics and Electrical Insulation*, vol. 23, pp. 1862-1871, 2016.
- [14] G. He, Q. Hu, L. Shu, X. Jiang, Y. Liu, W. Wu, Y. Li, and H. Peng, "Impact of icing severity on corona performance of glaze ice-covered conductor," *IEEE Transactions on Dielectrics and Electrical Insulation*, vol. 24, pp. 2952-2959, 2017.
- [15] T. Wszolek, "Diagnostic symptoms of corona audible noise in continuous monitoring systems," *Archives of Acoustics*, vol. 36, pp. 151-160, 2011.
- [16] Y. Liu, J. Guo and J. Lu, "Audible noise spectrum characteristics of positive and negative wire in UHV corona cage," *Proceedings of the CSEE*, vol. 34, pp. 2976-2982, 2014. (in Chinese)
- [17] A. Fridman and L. A. Kennedy, *Plasma Physics and Engineering*. New York: Taylor & Francis Books, 2004.
- [18] *IEEE Standard Definitions of Terms Relating to Corona and Field Effects of Overhead Power Lines*, IEEE Standard 539, 2005.
- [19] State Grid, *Xiangjiaba - Shanghai ± 800 kV UHV DC Transmission Demonstration Project. UHV DC Transmission Demonstration Project. Volume of Engineering Design*. Beijing: China Electric Power Press, 2014. (in Chinese)
- [20] *Electroacoustics - Sound Level Meters-Part 1: Specifications*, IEC Standard 61672-1, 2013.
- [21] G. Du, Z. Zhu and X. Gong, *Fundamental of Acoustics*. Nanjing: Nanjing University Press, 2001. (in Chinese)
- [22] D. A. Bies and C. H. Hansen, *Engineering Noise Control: Theory and Practice*. New York: Spon Press, 2009.
- [23] U. Straumann, "Mechanism of the tonal emission from ac high voltage overhead transmission lines," *Journal of Physics D Applied Physics*, vol. 44, pp. 1-8, 2011.